2D Hydrodynamic modelling on part of Mahanadi Delta Region

Piyush K. Jaipurkar
March, 2014

IIRS SUPERVISOR
Dr. Praveen Thakur
Dr. Vaibhav Garg

ITC SUPERVISOR
Dr. Victor Jetten

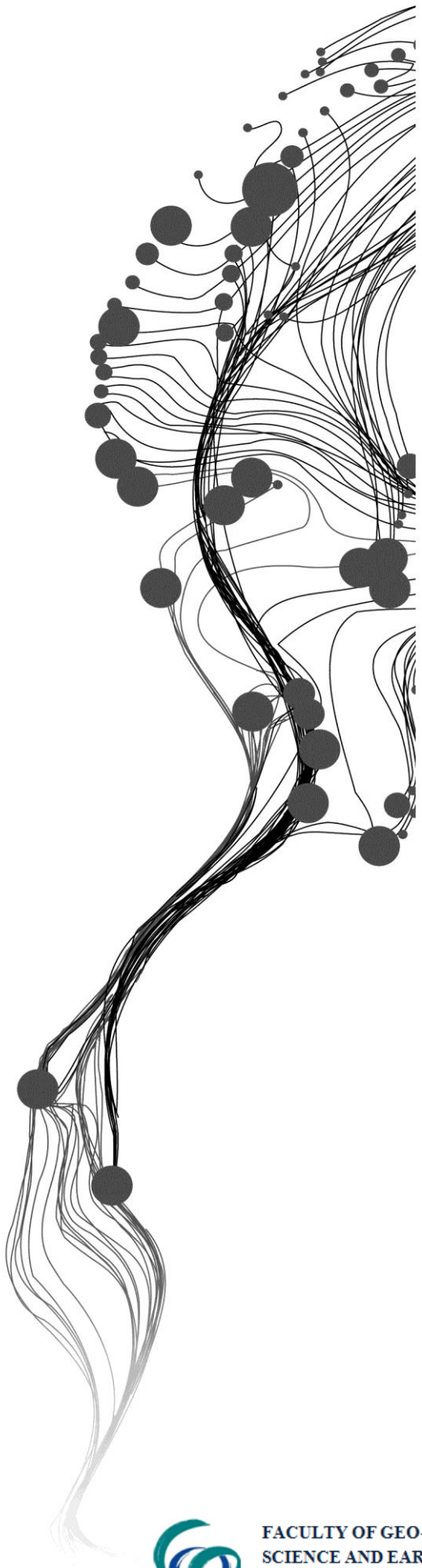

2D Hydrodynamic modelling on part of Mahanadi Delta Region

PIYUSH JAIPURKAR
Enschede, The Netherlands [March, 2014]

Thesis submitted to the Faculty of Geo-information Science and Earth Observation (ITC) of the University of Twente in partial fulfilment of the requirements for the degree of Master of Science in Geo-information Science and Earth Observation.
Specialization: Natural Hazards and Disaster Risk Management

THESIS ASSESSMENT BOARD:

Chairperson	: Dr. Alfred Stein
External Examiner	: Dr. S.K. Jain, NIH, Roorkee
Supervisors	: Dr. Praveen Thakur, IIRS
	Dr. Vaibhav Garg, IIRS
	Dr. Victor Jetten, ITC

OBSERVERS:

ITC Observer	: Dr. N.A.S. Hamm
IIRS Observer	: Dr. P. K. Champati Ray

FACULTY OF GEO-INFORMATION SCIENCE AND EARTH OBSERVATION, UNIVERSITY OF TWENTE, ENSCHEDE, THE NETHERLANDS

INDIAN INSTITUTE OF REMOTE SENSING
Indian Space Research Organisation
Department of Space, Government of India

DISCLAIMER

This document describes work undertaken as part of a programme of study at the Faculty of Geo-information Science and Earth Observation (ITC), University of Twente, The Netherlands. All views and opinions expressed therein remain the sole responsibility of the author, and do not necessarily represent those of the institute.

Dedicated to-

-My Family-

Mom, Dad,

Amit Dada and Sumit Dada

ABSTRACT

Disasters are considered uncontrollable events which interrupt essential functioning of society. Flooding is one such disaster. It is simply the overflow of water that submerges the land. Its occurrence is usually the aftermath of meteorological events. These include intense, prolonged rainfall, unusually high coastal and estuarine waters due to storm surges, etc. Structures situated in this flood plain are damaged due to floods. Flood modelling plays an important role in hazard mapping and risk assessment. It can be effectively used as mitigation tool. But its reliability depends on the quality of data required. The main input of any flood models is topographic data. Other than that it requires gauge discharge data and Land use Land cover map, etc. There are various techniques to available to acquire topographic data. These techniques produce data of various qualities which give different effect on modelling results. The study has been conducted on 18.3 km long reach of Dhanua River, located in part of Mahanadi Delta Region. During high discharge in Kushabhadra River, excess water is diverted to Dhanua through Jogisahi Escape. This diverted discharge at the time of Sep. 2003 flood event is calculated using discharge measurements from Balianta Gauging Station in HEC-RAS. This discharge was given to Dhanua River in 2D hydrodynamic model 'Lisflood-fp' to predict inundation. The study showed that as resolution gets coarser, the easiness of inundation along floodplain increases. Among the freely available topographic data, inundation shown using SRTM DEM was having highest overlap. It's overall accuracy and fit was measured as 65% and 37% resp. Unlike other freely available topographic datasets it is corrected for various voids. These missing values were calculated using algorithm called TOPOGRID which is specifically used to produce hydrological sound DEM.

Keywords: Hydrodynamic modelling, Lisflood-fp, Cartosat-1, DEM

ACKNOWLEDGEMENTS

I consider myself extremely fortunate for getting the opportunity of working under the valuable guidance of **Dr. Victor Jetten**, Professor and Head of Department of Earth Systems Analysis (ITC, Netherlands), **Dr. Praveen Thakur**, Scientist SE (IIRS, Dehradun, India) and **Dr. Vaibhav Garg**, Scientist SD (IIRS, Dehradun, India). They provided the conceptual and theoretical background of this study as well as suggested the rational approach. They remained a pillar of help and understanding throughout this project. Without the due attention and interest of them, this study could not have attained the last stage. We are also thankful for him for providing the necessary facilities for the project.

I also express my deep sense of gratitude to **Dr. S. P. Aggarwal**, Scientist SF and Head of Water Resources Department (IIRS) for providing all necessary facilities for completion of this project.

I am thankful to **Dr. S. Salama, W.J. Timmermans, J. Timmermans, C. van der Tol, R. van der Velde, L. Wang, Dr. Bhaskar Nikam, Ashutosh Bharadwaj** for help during different stages of this study.

I also want to thank Anil Kumar Kar, of Flood Management Cell, WRD, Orissa and Surojit Ghosh (JRF)for accompanying me in field visit.

I am also thankful to Col. S. Mohan Sir, Mr. Manjan (Ph.D. students), Shishant, Soumya, and other lab-mates for their timely cooperation, sympathetic nature throughout the study.

I also thank to friends Ishaan, Akhil, Arvind, Hemlata, Tanya, Ravisha, Kanishk, Guru and all for support. It was a small family away from home.

Without forgetting I also want to thank my friends in ITC friends Hervey from Rwanda, Irvan from Indonesia, Amro from Egypt all my class mates of Module 12 & Module13

My heartily thanks to PGD friends Ramanuj Kaushik, Manish Sir, Gangesh, Himanshu and all for co-operation in studies.

We can't forget to express our deep sense of respect towards our parents, Amit dada and Sumit dada. Without their blessing it would not have been possible for me to complete this project work.

Our hearty thanks are due to those who helped us directly or indirectly during my MSc program, whose names do not appear due to short of space or through oversight.

Dehradun, March 2014

Piyush K. Jaipurkar

TABLE OF CONTENTS

LIST OF FIGURES

LIST OF TABLES

1. INTRODUCTION

1.1. Background

Globally, the frequency of occurrence of natural disasters is increasing as seen in Figure 1. They include the severe acute respiratory syndrome (SARS) outbreak (2003), Hurricane Katrina (2005), the South Asian tsunami (2004), the swine flu pandemic (2009), the earthquake in Abruzzo, Italy (2009), and Japan's earthquake and tsunami (2011) and so on. Disruptions from these and other disasters have rippled across supply chains; shaken various industries; and have severely affected employee, customer, and partner relations. As a result of such dramatic events governments and economic agents are considering crisis preparedness and crisis management as key components of policy and business planning. (Sciusco 2012) Flooding is one of such disasters.

Frequency of flood occurrence is increasing all over the globe since 1970 (Guha-Sapir, Vos et al. 2011). It is basically a hydrological phenomenon and its occurrence is usually the aftermath of meteorological events. It may even occur due to human activities as well such as mismanagement of hydraulic structures and earth moving activities.

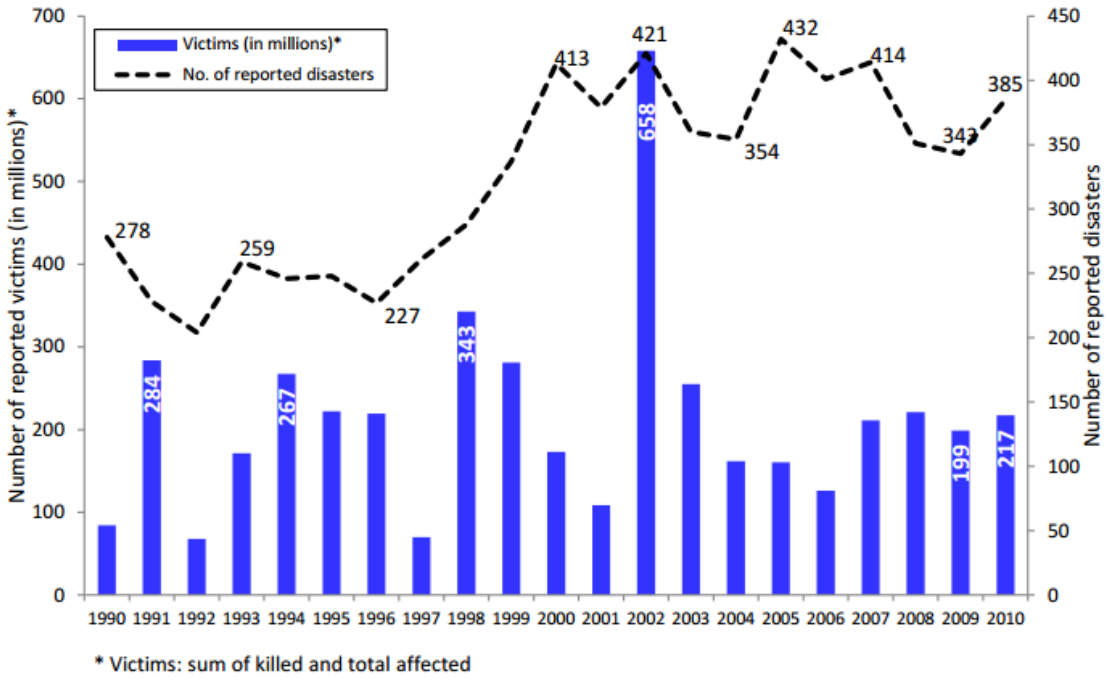

Figure 1: Trend and occurrence of disaster events and victims (Guha-Sapir, Vos et al. 2011)

Floods can be classified as minor and major flooding according to their extent and magnitude. In a minor flooding floodwaters are usually confined to the flood plain along the channel. Floodwater is usually shallow and there may not be a perceptible flow. When there are serious breaks in dams, embankments or other hydraulic structures, major floods are caused. Excess or uncontrollable discharge of water in reservoirs, lake, or rivers may also cause major floods.

Intensive rainfall over the catchment of river may also cause severe flood in lower catchment. This takes about 12 to 24 hours or even longer depending on distribution of rainfall and extent of catchment. When the time duration between rainfall and flood is six hours or less then it is known as flash floods. This rapid development of flood is due to extremely short concentration time drainage catchment. They also cause muddy flow by carrying away the soil, sediments and bed load.

Occurrence of flood is increased now days and especially in India as shown in Figure 2. Flash flood occurred in Kedarnath (Uttarakhand, India), flood due to Phailin cyclone in Orissa, India and recent floods Thames River in United Kingdom are apparently expressing the same. When such floods occur in populated area, they prove to be more destructive. Flood affects the generation and transmission of essential entities like water, electricity, etc. It also disrupts the sewage disposal system. This creates shortage of potable water and increases risk of waterborne diseases like typhoid, cholera. Due to disrupted transportation and bad weather, it becomes difficult to carry out relief operations.

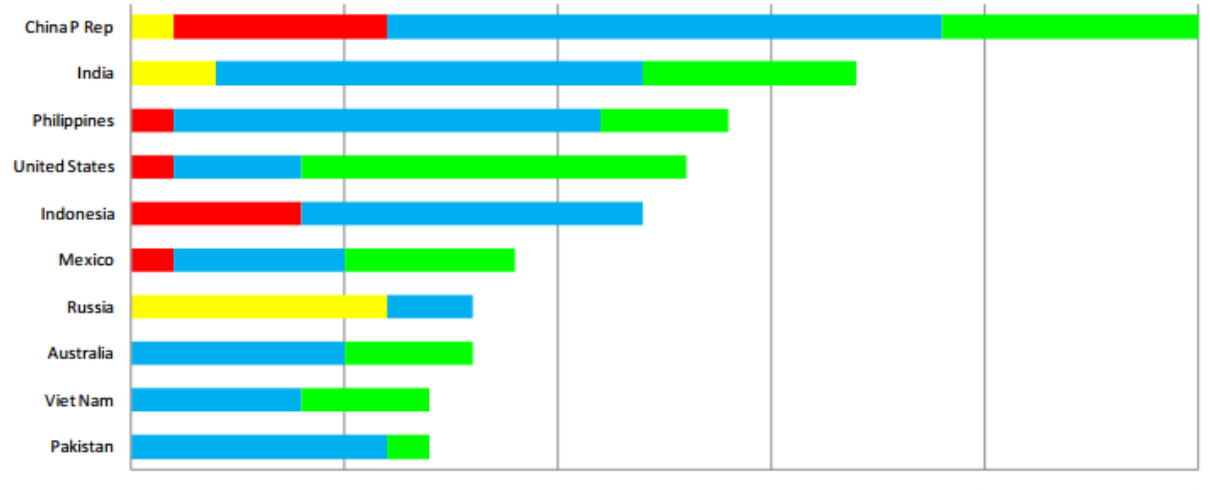

	China P Rep	India	Philippines	United States	Indonesia	Mexico	Australia	Russia	Pakistan	Viet Nam	Total
Climatological	1	2	0	0	0	0	0	6	0	0	9
Geophysical	5	0	1	1	4	1	0	0	0	0	12
Hydrological	13	10	10	3	8	4	5	2	6	4	65
Meteorological	6	5	3	9	0	4	3	0	1	3	34
Total	25	17	14	13	12	9	8	8	7	7	120

Figure 2: Top ten countries by no. of reported events (Guha-Sapir, Vos et al. 2011)

Structures and occupation situated in this flood plain have risk of damage due to floods. This damage can be reduced by moving them out of probable flood risk zone. The common source of flood is excess rainfall in high elevation area of basin. This excess water flows down to low elevation area to cause flooding.

Various mitigation measures can be taken to reduce the impact of floods like changing the way of flow to lower catchment so that high discharge flow is allowed to pass without causing floods. (Sushanta Kumar Jata 2011). This can be done if we have information about characteristics of flood propagation such as water depth, velocity, duration of flood and flood extent. Such kind of information can be obtained from various hydrodynamic inundation models.

Flood modelling also plays an important role in risk assessment. In the context of short-term decision-making, hydraulic modelling enables real-time now casts and/or forecasts that can be used for emergency management purposes such as evacuation, adaptive traffic management, and deployment of first responders and other

emergency personnel. However, this mandates models capable of completing 12–24 h flood forecasts in a few hours or less. (Sanders, Schubert et al. 2010)

The main input of any flood forecasting models is topographic data. This data is acquired using different techniques like photogrammetry, interferometry, aerial or terrestrial laser scanning. These techniques produce data of various resolutions and quality. They have different effect on modelling results. It ultimately affects the mitigation work.

Various authorities are using contemporary, commercial hydrological models for flood modelling and forecasting purpose. Use of freely available models will be reducing the cost for flood management and rescue operations. Hence, 'Lisflood-fp' model was used in the project work. It is also used since its compatibility with results of other rainfall runoff model like VIC. The topographic data required can be produced by using Cartosat stereo pairs which comparatively cheaper. By effective use of such low cost resources hydrodynamic modelling can be done. This will be very useful tool for small city and towns' administration to predict and mitigate the disaster as well as for risk assessment.

This study will deal with use of hydrodynamic model, GIS and remote sensing to model flood inundation. It will later calibrate and validate the model for topography of part of Mahanadi delta region.

1.2. Objectives

- To perform raster based flood inundation modelling on part of Mahanadi Delta
- To what extent inundation maps generated by model are dependent on resolution DEM used

1.3. Research Questions

Research Questions to be answered are as follows-

- What is the accuracy of model simulations with SAR data?
- What are the changes in simulated inundation area due to change in DEM of different resolution?

2. STUDY AREA

2.1. Mahanadi Delta Region

Mahanadi river basin is spread over 141589 sq. km. It is about 4.3% of total geographic area of India. The Maximum portion of basin is over Chhattisgarh and Orissa. Small portion of basin is in other three surrounding state. This basin geographically lies within $80^0$28' and $86^0$43' east longitudes and $19^0$8' to $23^0$32' north latitudes. Basin has length and width of 587km and 400km. It is surrounded by hills in central India, Maikala Range from west and Eastern Ghats on south and east. Its description is shown in Table 1.

Mahanadi is a major river in India located in peninsular region of country. It ranks ninth in India, in terms of water potential and flood producing capacity. (WRIS 2012)

The study area is limited to Mahanadi delta region after the Mundali gauging station as shown in the Figure 3 below.

Table 1: Salient Features of Mahanadi Basin (WRIS 2012)

Salient Features of Mahanadi Basin	
Basin Extent	
Longitude	$80^0$28' to $86^0$43'E
Latitude	$19^0$8' to $23^0$32' N
Length of Mahanadi river (Km)	851
Catchment Area	141589
Average Water resource Potential (MCM)	66880
Utilizable Surface water resources (MCM)	50000
No. of Hydrological observation stations	39
No. of flood forecasting stations	4

2.2. Study Area

The study area is spread to extent of $20^0$16' 51" to $20^0$8' 53" North and 85^0 51' 44" to 85^0 58' 31" East. It contains spill way called 'Jogisahi Escape' which diverts excess water through artificial flood inundation channel called 'Dhanua River'. Image of field photograph is shown in Figure 4 and Figure 5. It was constructed to save urban area along Kushabhadra River from getting flooded. There are various causeways (Figure 6) used for

transportation which are closed during the flood period. From past few decades this area is extensively used for agricultural purpose.

Due to frequent deposition of sediments from flood, this land has become very fertile. Hence it is extensively used for farming. It can be seen from field photographs in from Figure 7. If we are able to forecast flooding in this land it will be helpful for farmers and labourers to reduce the loss. They can harvest the standing crops before it gets destroyed by flood water. It will also serve as warning to labours to vacate the floodplain area.

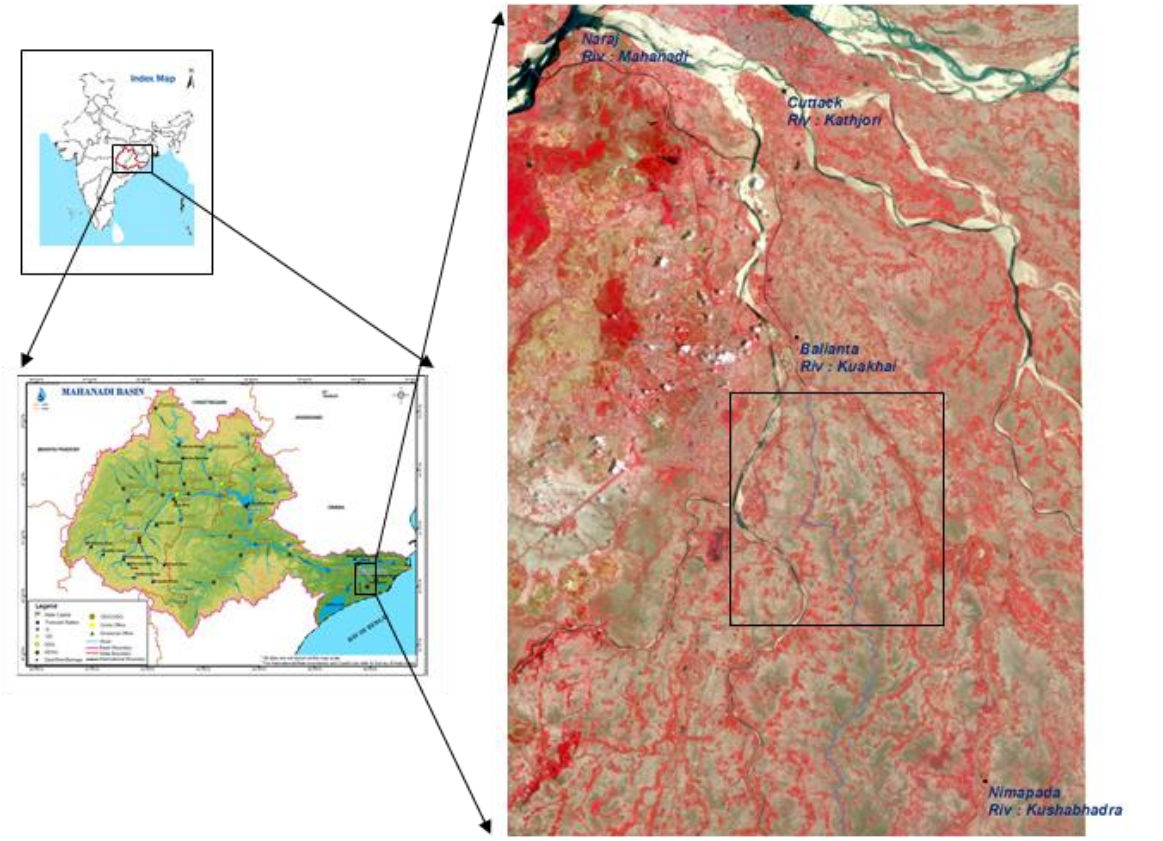

Figure 3: Dhanua River (in blue colour), Various Gauging stations in study area shown over Liss-3 Multi-spectral Image. Location of study area is incited in map of Mahanadi river Basin in left bottom corner. Location of Mahanadi Basin is shown in Map of India.

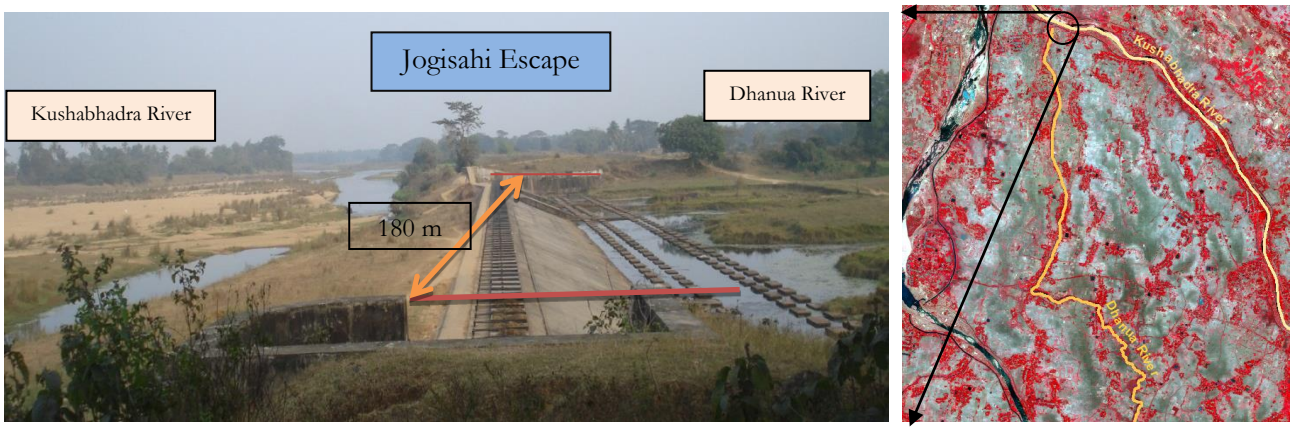

Figure 4: Jogisahi Escape. At right side Kushabhadra River. During flood period excess water in Kushabhadra River is diverted to Dhanua River through this structure. It's length was measured to be 180m. Image was taken during field visit by Piyush Jaipurkar and Surojit Ghosh on 15th Jan 2014

Depth provided in the escape was measured to be 2.3 meter. Hence from the image 2 the height of structure above ground can be approximated to be 4.6 meter. It has slope of about 0.148 m/m.

Figure 5: Height Measurements on Jogisahi Escape. Image was taken during field visit by Piyush Jaipurkar and Surojit Ghosh on 15th Jan 2014.

Figure 6: Causeway over Dhanua River: They are constructed for transportation across river. Due to low elevation they remain closed during flood. Image was taken during field visit by Piyush Jaipurkar and Surojit Ghosh on 15th Jan 2014.

Figure 7: Upstream view of Dhanua River from Causeway. Image was taken during field visit by Piyush Jaipurkar and Surojit Ghosh on 15th Jan 2014.

3. LITERATURE REVIEW

Recently researchers are using hydrodynamic modelling to study flood inundation over floodplain. (Werner 2004, Bates PD 2005). Various numerical models have been developed for flood inundated area delineation. This is further used to determine risk zones for flood having various return periods. These numerical models can be classified as (1) one-dimensional (1D) models, (2) two dimensional (2D) models, (3) one-dimensional river flow models coupled with two-dimensional floodplain flow (1D-2D) models, and (4) numerical models trying to accurately describe the hydraulic resistance of a vegetated floodplain and describe the fully 3D velocity (3D)(Stoesser, Wilson et al. 2003)

1D model are simple and inform about bulk flow characteristic. For getting details about flood inundation, attempts were made to develop 1D, 2D and 3D models like MIKE 21, DELFT-FLS, SOBEK, RMA-10 and DELFT-3D.

3.1. 'Lisflood-fp' Model Description

- Lisflood-fp is raster based storage cell flood inundation model. It is a simple coupled 1D/2D model. It's main objective was to combine best features of 1D and 2D models (Bates and De Roo 2000). It has 1D representation of channel which used either kinematic, diffusive or sub grid channel solver. (Trigg, Wilson et al. 2009). (Neal, Schumann et al.) It is freely available and used as research tool within the pre-operational European Flood Alert System (EFAS) being developed by Dr. Ad De Roo at the EU Joint Research Centre.

All channel solvers are based on continuity equation.

$$\frac{\partial Q_c}{\partial x} + \frac{\partial A}{\partial t} = 0 \qquad 1$$

In above equation, 'Q_c' is volumetric flow (m^3/sec), 'x' is distance down slope (m), 'A' is cross section area of flow (m^2), and 't' is time (sec).

Kinematic channel solver use shallow water equations in which only friction and bed gradient are considered else neglected. In terms of momentum eq. it is represented as:

$$\frac{\partial z}{\partial x} - \frac{n^2 P^{4/3} {Q_c}^2}{A^{10/3}} = 0 \qquad 2$$

Symbols are same as that of before in addition 'z' is bed elevation (m), 'n' is Manning's coefficient of friction (unit less) and 'P' is wetted perimeter of flow (m).

Diffusive channel solver is similar to kinematic just one more term of free surface slope is considered. It momentum eq. can be written as:

$$\frac{\partial z}{\partial x} - \frac{n^2 P^{4/3} {Q_c}^2}{A^{10/3}} - \left[\frac{\partial h}{\partial x}\right] = 0 \qquad 3$$

Kinematic Terms Diffusion Term

Symbols are same as above in addition of 'h' is flow depth (m). In above two methods channel is discretised as a single vector along its centreline separate from raster DEM.

In sub grid channel solver, channel of any size less than the resolution of grid can be represented. Figure 8 represents conceptual diagram of base model and subgrade model. (Neal, Schumann et al.)

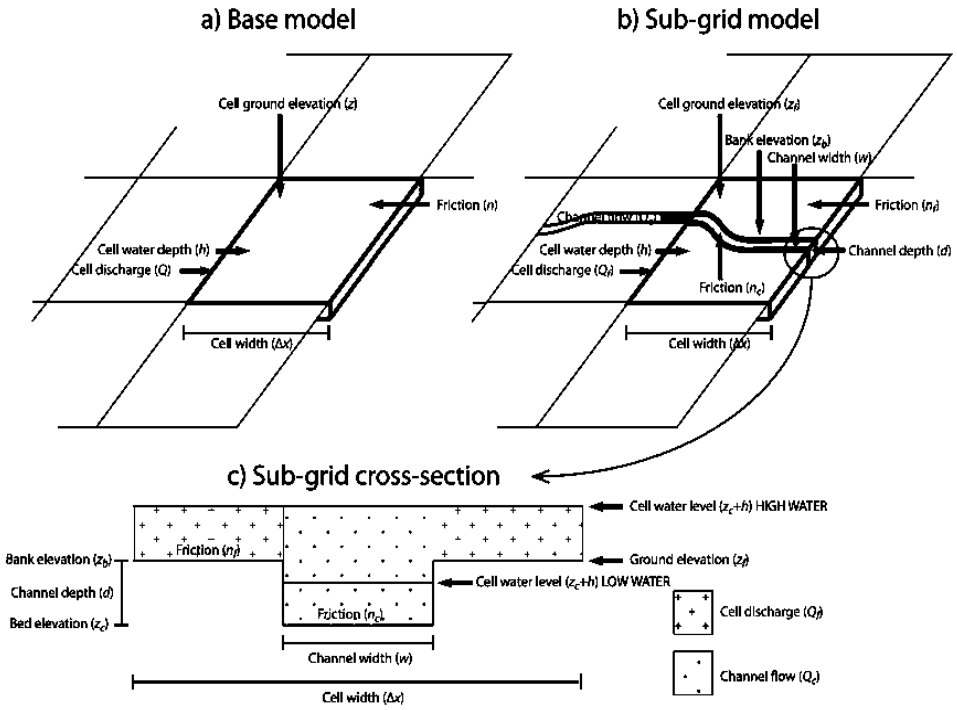

Figure 8: Conceptual diagram of (a) 'lissflood-fp' base model, (b) sub grid channels model, and (c) sub grid section

For flood plain modelling it uses a simple storage cell algorithm. In this it calculates the water level of orthogonally adjacent cells for each time step as shown in Figure 9. In this way it calculates water level for each cell of DEM in each time step. For detailed explanation refer to (Bates and De Roo 2000)

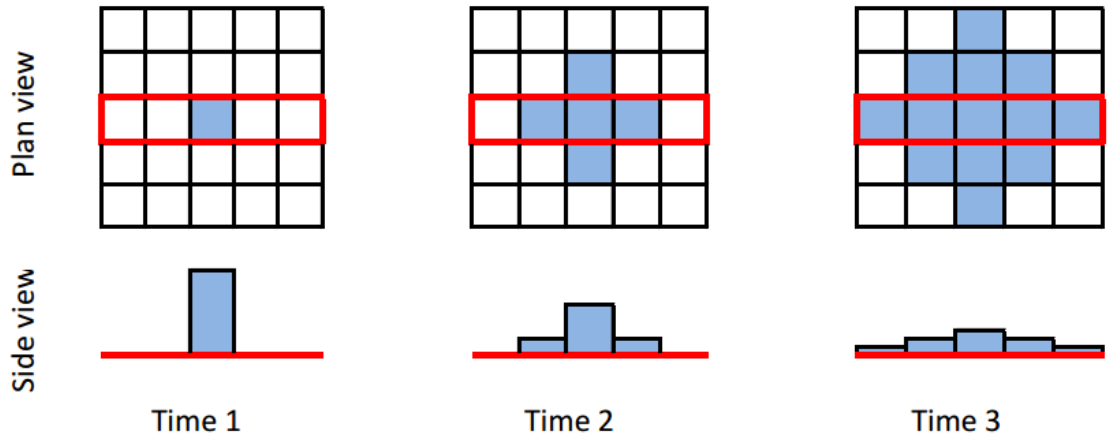

Figure 9: Two-dimensional diffusion representation of floodplain flow (adapted from Willson 2011)

3.2. Lisflood-fp model Applications

The model was basically developed to harness the potential of high resolution remotely sensed data. This newly developed model was applied on 35 km reach of the River Meuse in The Netherlands for the flood event of January 1995. It was validated using SAR data and airborne imagery. The predictions of model were 81.9% correct.(Bates and De Roo 2000)

In study conducted by Horritt and Bates different resolution DEM varying from 10m to 1000 m resolution were tested and compared. It found that 100m resolution image was giving stable result when model was calibrated against observed inundated area. Further decreasing the resolution was not showing any significant improvement. For prediction of water level 500m resolutions DEM was yielding adequate results. It was seen that model cannot be calibrated to get acceptable wave travel time and inundation period.(Horritt and Bates 2001)

Horritt and Bates have done a comparative study of raster based inundation model LISFLOOD-FP with generalized finite element model TELEMAC-2D. They validated both the models with flood inundation extent obtained by SAR imagery. They also calibrated the model for friction parameter at which predicted and observed inundation areas are most similar. The result of their comparison was that both models were giving similar results. There was not any significant difference in the performance of models. This was due to errors in validation data i.e. SAR imagery. The raster based model LISFLOOD-FP was advantages regarding calibration. It also has flexibility for specification of channel as compared to finite element model TELEMAC-2D.(Horritt and Bates 2001a)

Raster-based storage cell codes have many of the advantages over full two-dimensional models but require complex computation. However it implementation has some complex limitations. These make it incapable to develop solutions that are independent of time step or grid size, and an unrealistic lack of sensitivity to floodplain friction. The solution to these problems based on an optimal adaptive time step determined using the Courant–Freidrichs–Levy condition for model stability are analysed in (Hunter, Horritt et al. 2005). Comparison of adaptive time step scheme to analytical solutions of wave propagation on flat and sloping planar surfaces shows considerable improvement over a standard raster storage cell model. Moreover, this scheme showed results that are independent of grid size or choice of initial time step and which show an intuitively correct sensitivity to floodplain friction over spatially complex topography.

Here Bates and Wilson used high resolution airborne SAR data and high resolution LASER altimetry data of high vertical accuracy to validate the model. This facilitated to calculate dynamic changes in inundation area, total reach storage and rates of reach dewatering. (Bates, Wilson et al. 2006)

Hydrodynamic modelling of Amazon was done at large spatial scale in (Wilson, Bates et al. 2007). They used topographic data from the Shuttle Radar Topography Mission in Lisflood-fp model to predict flood plain inundation of 240 × 125 km section. They did validation with satellite derived flood extent, gauge data and satellite altimetry. They found that accuracy of model at high water is 72% in spatial fit and 0.99m RMSE in water stage height. While at low water it was 23% in spatial fit and 3.17m RMSE in water stage height. This sharp drop was due to due to incomplete drainage of the floodplain. These are due to errors in topographic data. Work of (Trigg, Wilson et al. 2009) further studied the hydraulic characteristics of the Amazon flood wave.

In (Hunter, Bates et al. 2008), a massive work of comparing various 2D hydraulic models (DIVAST, DIVASTTVD, TUFLOW, JFLOW, TRENT and LISFLOOD-FP) was carried out under similar conditions of

densely urbanised area. For this they considered 4 km urban catchment within the city of Glasgow, Scotland, UK and used data of flood event that occurred at that site on 30 July 2002. In particular, the results of this study showed terrain data available from modern LiDAR systems are sufficiently accurate and resolved for simulating urban flows, but such data need to be fused with digital map data of building topology and land use to gain maximum benefit from the information contained therein. Once it is available uncertainty in friction factor becomes more governing factor. The simulations also showed that flows in urban environments are characterised by numerous transitions to supercritical flow and numerical shocks.

Yamazaki has shown the importance of quality of DEM in hydrological modelling. In this they have developed an algorithm to remove pits in space born DEM. Such pits are caused due to vegetation canopies, sub-pixel sized structures and random radar speckles.(Yamazaki, Baugh et al. 2012)

A large scale flood inundation forecasting was also carried out by using Lisflood-fp model. (Schumann, Neal et al. 2013). This study was carried out at Lower Zambezi River to demonstrate current flood inundation forecasting capabilities in large data-scarce regions. Here they used newly developed sub grid channel scheme to describe river network. Model evaluation showed that simulated flood edge cells were within a distance of between one and two model resolutions compared to an observed flood edge and inundation area was accurate about an average of 86%.

3.3. Related studies DEM, Study area and its effect

Topographic data is most important component of any 2D hydrodynamic modelling. It is very critical for delineating flood inundation extent. In (Aaron Cook 2009), effect of topography, geometric configuration and modelling approach on two different study area has been addressed. It found that inundation area decreases as the resolution and vertical accuracy of topographic data increases. In most of the elevation data bathymetric data is not included. After including actual bathymetric data in modelling, it was found that inundation area decreased significantly. In 1D model if number of cross sections is increased then larger area gets inundated. If structural details like bridges and culverts are not considered then no effect will be seen on large scale but localised inundation is wrongly represented. FESWMS (The Finite Element Surface Water Modelling System) was used by them generated less inundation area as compared to HEC-RAS. Variation in inundation extent with respect to resolution is less in FESWMS then HEC-RAS. All its findings conclude that 2D modelling approach is more realistic then 1D approach.

Since, DEM is very sensitive component of 2D hydrodynamic modelling its accuracy has to be assessed. A study was carried out by (Mukherjee, Joshi et al. 2013) to evaluate vertical accuracy of open source Digital Elevation Model. In this study they evaluated ASTER and SRTM DEM and their derived attributes using high postings Cartosat-1 DEM and Survey of India (SOI) height information. Accuracy calculated by them show RMS error of 1.62m and 17.76m for ASTER and SRTM respectively in comparison with Cartosat-1 DEM. The slope and drainage network were also not in good agreement.

The 2D and 3D models require bathymetric information and floodplain elevation information in continuous surface. Various issues associated with creating an integrated river terrain is disused in (Merwade, Cook et al. 2008) and GIS technique is proposed to overcome these issues.

4. MATERIALS

4.1. Digital Elevation Model

ASTER, SRTM, Cartosat-1 stereo pairs were used shown in Figure 10.

The Advanced Space borne Thermal Emission and Reflection Radiometer (ASTER) DEM of version 2 for this study was obtained from http://gdem.ersdac.jspacesystems.or.jp/feature.jsp. It's vertical accuracy was reported as 17.01m at 95% confidence level by ASTER GDEM Validation results released on August 31, 2011.(Tachikawa, Kaku et al. 2011)

Shuttle Radar Topography Mission (SRTM) DEM v4.1 was obtained from 'http://www.cgiar-csi.org/data/srtm-90m-digital-elevation-database-v4-1'. It is provided by NASA for large portions of the tropics and other areas of the developing world. It is high quality elevation data having vertical accuracy of less than 16m with 90% confidence level. (Rexer and Hirt 2014)

CartoDEM was obtained from 'http://bhuvan-noeda.nrsc.gov.in/'. This was developed by the Indian Space Research Organization (ISRO). It was derived from the Cartosat-1 stereo payload launched in May 2005. It's elevation accuracy was measured as 8m with 90% confidence level as. (Muralikrishnan, Pillai et al. 2013)

Cartosat Stereo DEM was also produced from panchromatic images of Cartosat-1. These images were acquired on date 23 Jan 2012. Path and row of sensor is 580 and 303. The DEM was generated by using RPC files and evenly distributed tie points in DEM extraction wizard of ENVI 5.0. It must be noted that only three GCP's were used. Hence, its accuracy is compromised.

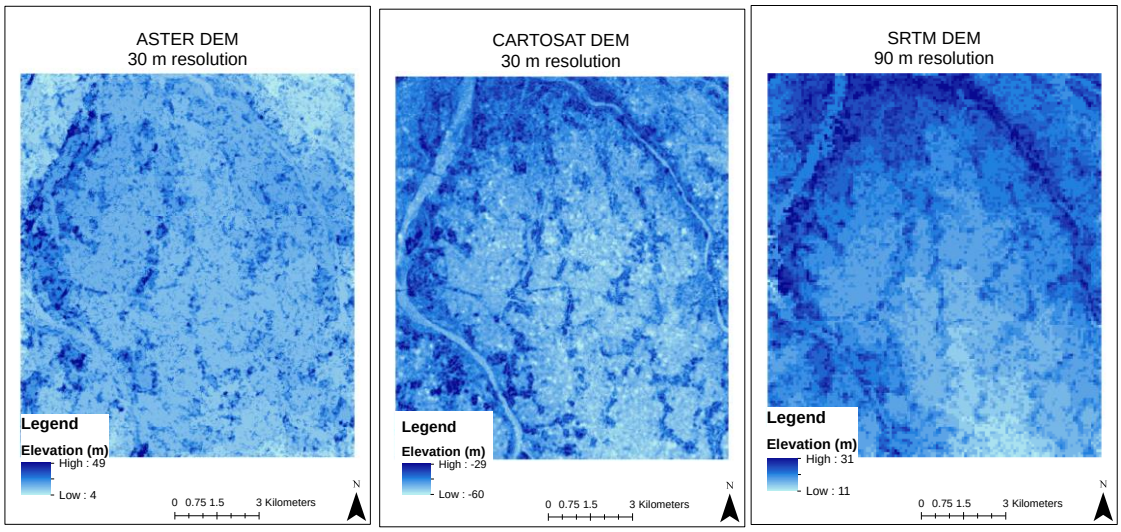

Figure 10: ASTER of 30m resolution, Cartosat DEM of 30m resolution and SRTM of 90m resolution.

4.2. Boundary conditions

The hourly discharge data is available at Balianta Gauging station situated on Kushabhadra River. It was collected by hydrometry Department. During high flood excess discharge is diverted in Dhanua River through Jogisahi spillway. This diverted discharge is not measured by any governmental or non-governmental departments. It was calculated by using HEC-RAS (Hydrologic Engineering Centers River Analysis System). The hydrographs of discharge at Balianta gauging station and Jogisahi escape are shown in Figure 11.

Boundary conditions at all edges were kept as free i.e. water will move out of the extent of the DEM without any water-depth restrictions.

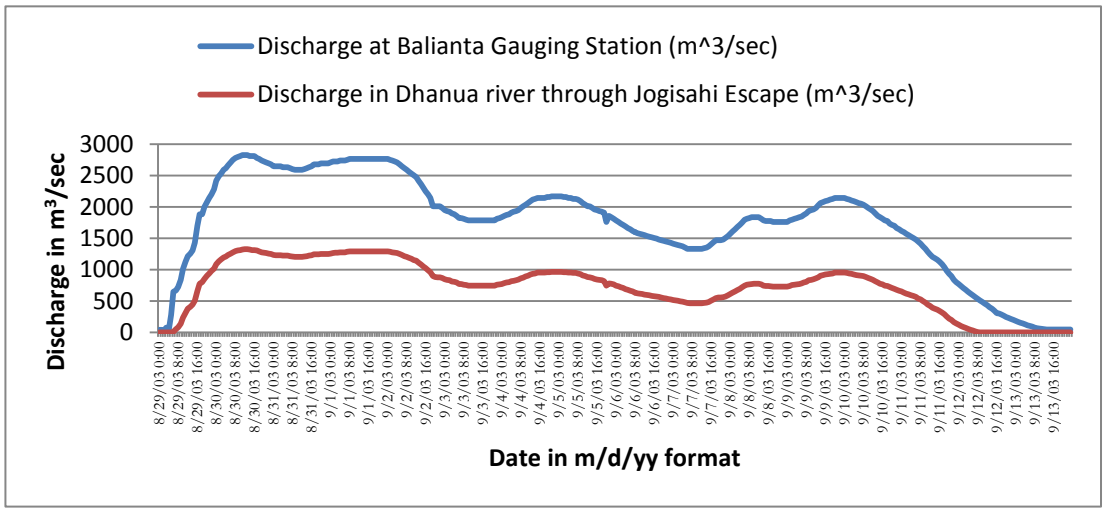

Figure 11: Hydrograph of Discharge in Kushabhadra River (from gauging station) and the same for Dhanua River (derived from HEC-RAS) for period from 29th Aug 2003 to 13th Sep 2003

4.3. Liss IV –MX Multi-Spectral Image

An image from Liss IV sensor in MX mode was acquired on Feb '12. It is an optical, multispectral image of 5.8 m resolution. It's one scene has an extent of 23.9 km X 23.9 km. Spectral Range for each band range is shown in Table 2. Image of Liss IV MX to the extent of study area is shown in Figure 12.

Table 2: Spectral Bands of Liss-IV MX sensor

Band name	Band [µm]	Code	Maximal resolution [m]
MX Mode 2	0.52 – 0.59	GREEN	5.8
MX Mode 1	0.62 -0.68	RED	5.8
MX Mode 4	0.77 – 0.86	NIR	5.8

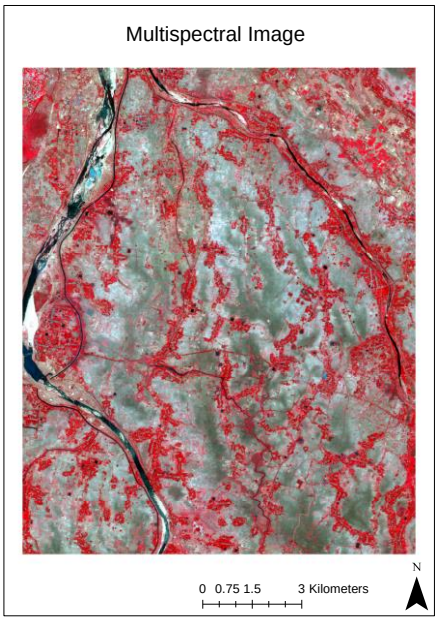

Figure 12: Multispectral Image of Liss IV sensor in MX mode

4.4. Radarsat-1 Microwave Image

Microwave Image was obtained from Radarsat-1 was used for validation of inundation predicted by model. Radarsat-1 was launched by Canadian Space Agency (CSA) in sun synchronous orbit. The product provided by them is having coverage of 500 km x 500 km. This data was acquired with frequency 5.3 GHz and wavelength of 5.6cm (c-band), R.F bandwidth 11.6:17.3 or 300MHz and Antenna size 15.0x1.5m with Shift quantisation of 8 bit (http://www.asc-csa.gc.ca/eng/satellites/radarsat1). The acquisition was done on 4th Sep 2003 at 12hr 20 min 4.89 sec. Study area in SAR image is shown in Figure 13.

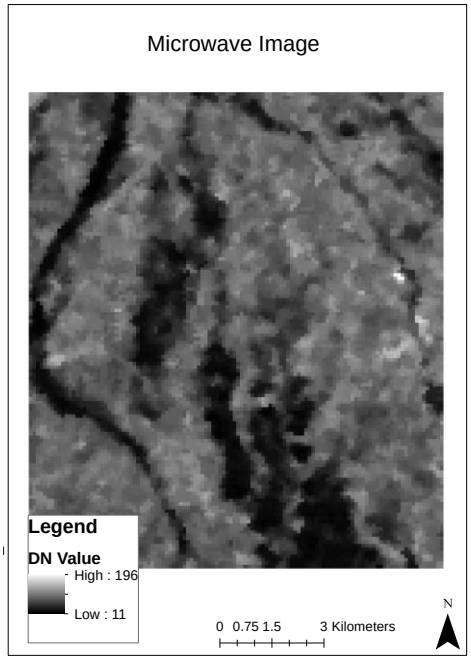

Figure 13: Radarsat-1 Image on over pass of 4th Sept '03 at 12hr 20min 5sec

4.5. Soil Map and Infiltration Rate

Soil map by NBSS&LUP (National Bureau of Soil Survey and Land Use Planning) was obtained. It showed that most of the area was covered by Loamy sand and small part is having clay. Soil Map is shown in Figure 14: Soil Map. Infiltration rate for various soil type at different slope were available on 'http://qcode.us/codes/sacramentocounty/view.php?topic=14-14_10-14_10_110&frames=on'. This information was made available by USDA (United States Department of Agriculture). The study area is mostly flat. For land having slope of 0% to 4% infiltration rate was given as 0.88 inch/hours i.e. 0.000006209 m/sec. This value was assigned uniformly over the complete flood plain.

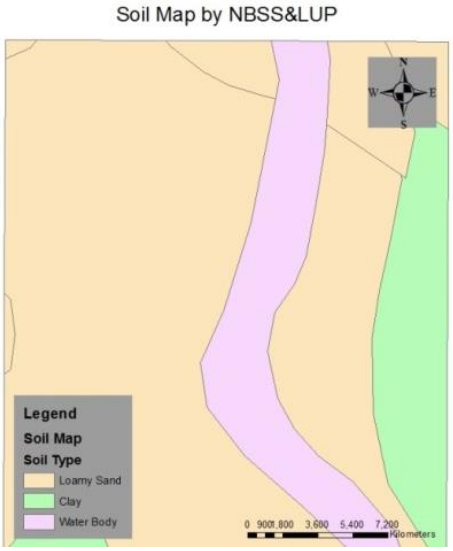

Figure 14: Soil Map by National Bureau of Soil Survey and Land Use Planning (NBSS&LUP)

4.6. Friction Factor

The friction factor for channel and flood plain was determined according to guidelines given in (Arcement and Schneider 1989).
The friction value for channel and flood-plain is calculated by:

$$n = (n_b + n_1 + n_2 + n_3 + n_4) \times m$$

In case of channel terms in above formula represents,
n_b= a base value of n for a straight, uniform, smooth channel in natural materials
n_1 =a correction factor for the effect of surface irregularities
n_2 =a value for variations in shape and size of the channel cross section
n_3= a value for obstructions
n_4= a value for obstructions
m= a correction factor for meandering of the channel

In case of flood-plain,
n_b= a base value of n for the flood plain's natural bare soil surface
n_1=a correction factor for the effect of surface irregularities on the flood plain
n_2 =a value for variations in shape and size of the flood-plain cross section is assumed equal to zero
n_3=a value for obstructions on the flood plain
n_4=a value for vegetation on the flood plain
m= a correction factor for sinuosity of the channel is assumed equal to one

Values for each term were determined after extensive interpretation of imagery and keen observation on field visit.

Table 3: Calculation of Friction Factor for Dhanua River

Symbol	Description	Observation of Dhanua River	Limits	Value Determined
n_b	a base value of n for a straight, uniform, smooth channel in natural materials	Stable Soil	0.025 to 0.032	0.025
n_1	a correction factor for the effect of surface **irregularities**	Minor Irregularities	0.001-0.005	0.001
n_2	a value for **variations in shape and size of the channel cross section**	Alternating Occasionally	0.001-0.005	0.002
n_3	a value for **obstructions**	Minor Obstruction	0.005-0.015	0.005
n_4	a value for **vegetation**	Medium	0.01-0.025	0.025
M	a correction factor for **meandering** of the channel	Severe	1.3	1.3
			Friction Factor for Dhanua River	0.0754

Table 4: Calculation of Friction Factor for Flood Plain

Description		Observation		Limits		Value determined	
		Rural Built-up	Agriculture/ Fallow land	Rural Built-up	Agriculture/ Fallow land	Rural Built-up	Agriculture/ Fallow land
Symbol	a base value of n for a straight, uniform, smooth channel in natural materials	Rock Cut or Firm Soil	Firm soil	0.011-0.020	0.02	0.011	0.02
n_1	a correction factor for the effect of surface **irregularities**	Severe	Moderate	0.011-0.020	0.006-0.010	0.011	0.01
n_2	a value for **variations in shape and size of the channel cross section**	Gradual	Gradual	0	0	0	0
n_3	a value for **obstructions**	Appreciable	Minor	0.020-0.030	0.005-0.019	0.02	0.005
n_4	a value for **vegetation**	Small	Very large	0.050-0.100	0.001-0.010	0.05	0.001
M	a correction factor for **meandering** of the channel	Not Applicable	Not Applicable	1	1	1	1
					Friction Factor for Flood Plains	0.092	0.036

As discussed above, there are three major land cover in flood plain viz. agriculture/fallow land, Rural Built-up and water body. Friction factor for water body is assumed equal to zero. The calculation for Rural built-up and agriculture/fallow land are determined below in following tables. The Values for each factor was determined on basis of images and observations of flood-plain and channel taken during field visit.

4.7. River data

Lisflood-fp model require width, friction factor, bed elevation and boundary condition at various geometric locations along the river. Width of river measured in field and from imagery came out to be 30m. It was fairly constant along the river reach. Friction factor calculated in Table 3 above as 0.076 was assumed to constant along the river reach. Bed elevation values for first and last location was taken as DEM and intermediate bed elevation values were linearly interpolated. At the first point hourly discharge data was given.

4.8. Software used

a) ArcGIS 10.1
b) Erdas IMAGINE
c) ENVI 5.0
d) Lisflood-fp
e) HEC-RAS

4.9. Solvers Used in Modeling

In literature review three channel flow solvers (viz. diffusive, kinematic and sub grid channel solvers) and three 2D floodplain flow solver (Flow limited, adaptive and acceleration) were discussed. In this study kinematic channel Solver and flow-limited floodplain solver were used. In kinematic channel solver initial time step was given of 100sec.

5. METHODOLOGY

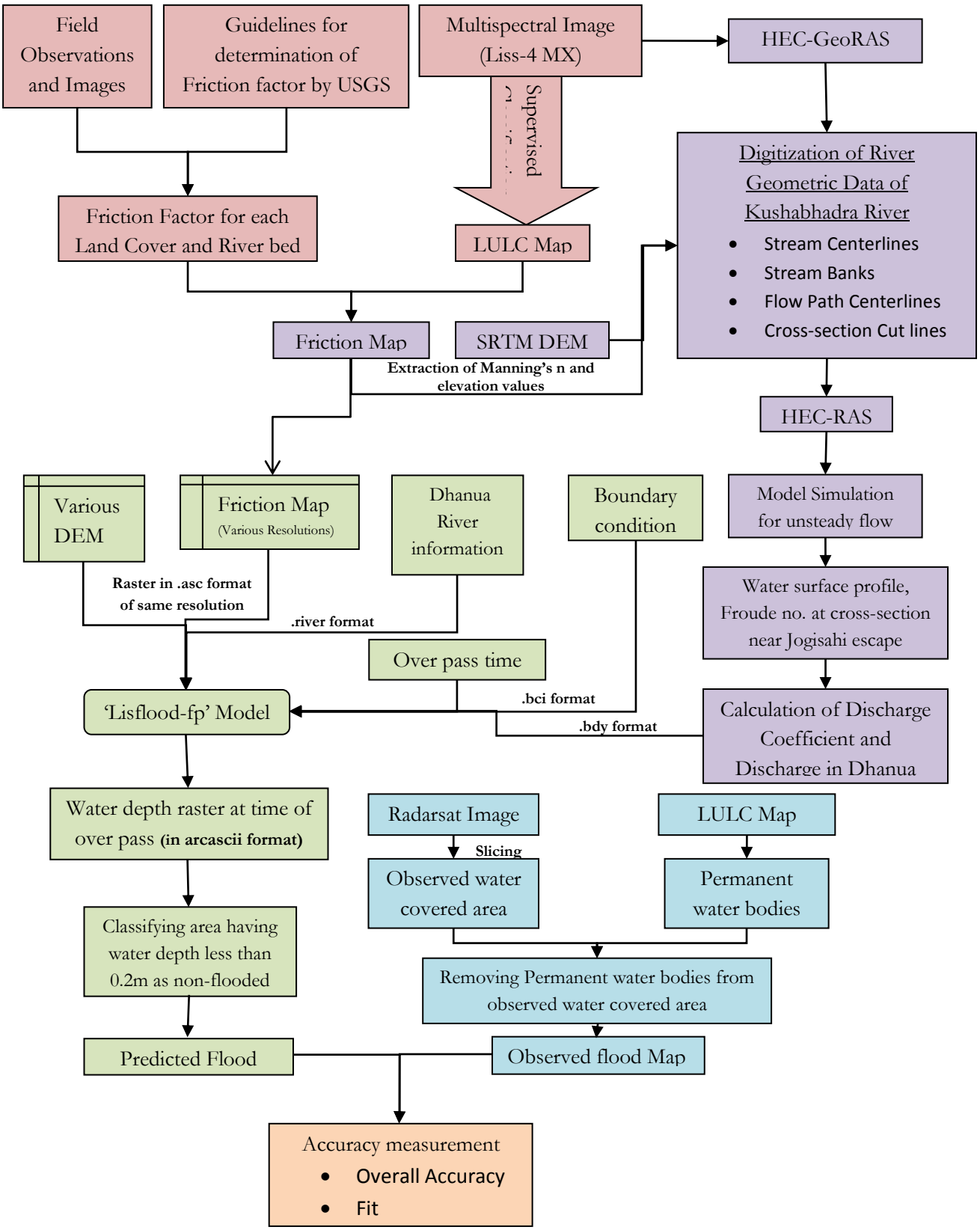

Figure 15: Schematic representation of Methodology: (1)Preparation of LULC Map and Friction Map (2) Calculation of Discharge in Dhanua River using HEC-RAS (3) Preparation of Predicted flood map using lisflood-fp model. This step is repeated using various DEM. (4) Preparation of Observed Flood Map using Radarsat Microwave Image. (5) Accuracy assessment using Fit value and Overall Accuracy

5.1. LULC and Friction Map

In terms of land use flood plain can be classified in to three major class agriculture/fallow land, Rural Built-up and water body. Supervised classification was done on LISS4-MX of period January of 2012. The Rural built-up are surrounded by trees. So, signature of trees was considered as Rural Built-up. There were small artificial lakes made all over the floodplain for agriculture purpose. These lakes and river signatures were taken as water bodies. The remaining area is agriculture/fallow land. Liss4 is shown in Figure 12. The LULC map prepared is shown in Figure 16. Classification accuracy was measured by taking 20 random points. The overall accuracy was calculated as 85%. Accuracy report is shown in Appendix 1. Friction factor for each flood plain type is calculated in Table 4. They are shown in Table 5.

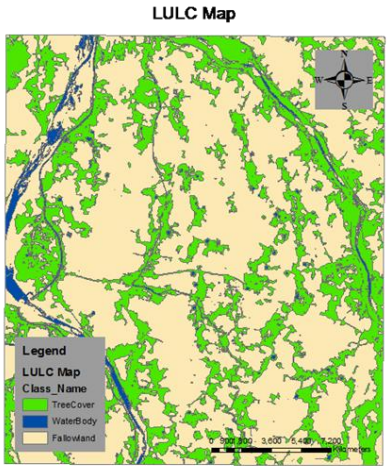

Figure 16: LULC Map prepared by performing supervised classification on Liss-4 MX Image

Table 5: Friction factor for flood plain of each land cover

Class Name	Flood-Plain Friction
Tree Cover	0.092
Agriculture/Fallow land	0.036
Water Body	0

5.2. Determination of discharge in Dhanua

Hourly Discharge at Balianta station on River Kushabhadra for period of 29 Aug 2003 to 13 Sep 2003 was available. This was used to get water surface elevation at the cross section at Jogisahi escape using HEC-RAS. The elevation of Jogisahi escape was subtracted. This gave water depth in meter ('d') flowing above Jogisahi escape. This is used to calculate discharge at Dhanua River.

Discharge flowing over side weir is calculated by using SVF (Spatially Varied Flow) Equation as follows-

$$Q = \frac{2}{3} * L * C_d * \sqrt{2g} * d^{\frac{3}{2}}$$

Where, Q is discharge (m^3/sec); L is length of weir (m); C_d is discharge coefficient (unit less) or De Marchi Coefficient; g is acceleration due to gravity (m/sec^2); and d is water depth (m) above escape. All units are in IS units. (Subramanya 2007)

C_d is calculated using equation suggested by Rangaraju for weir discharging at 90^0 to main channel.

$$C_d = (0.81 - 0.6F) * (0.8 + 0.1\frac{d}{L})$$

Where, F is Froude No. All other notations are as same as above. This equation is for broad crested weir discharging from main cannel to 90^0-branch cannel. (Subramanya 2007)

Froude no. is calculated by:-

$$F = \sqrt{\frac{{Q_{in}}^2 B}{gS^3}}$$

Where, Q_{in} is discharge along that cross-section (m^3/sec); B is top width of that cross section (m); g is acceleration of gravity (m/sec^2); and S is wetted perimeter of that cross-section (m). (Subramanya 2007) This was calculated by HEC-RAS.
The discharge so calculated is shown in following graph along with discharge used earlier.

5.3. Modeling with Lisflood-fp

Lisflood-fp model requires various inputs like DEM, Friction map, River data, boundary conditions, and discharge. In result it gives mass balance file. In this all maps has to be of same resolution. The elevation and width has to be in meters and discharge in m^3/sec. The water depth map produced by model will be used to map the inundated area. All input and output of Lisflood-fp model is shown in Figure 17. In predicted flood map, area having water depth less than 0.2 meters is considered as non-flooded. Similar predicted flood maps were prepared using DEM of various resolutions (like 6m, 10m, 20m, 30m, 60m and 90m produced using Panchromatic Cartosat-1 stereo-pairs). Along with them three other freely available (viz. Cartosat, ASTER and SRTM) DEM were also used to simulate Lisflood-fp model.

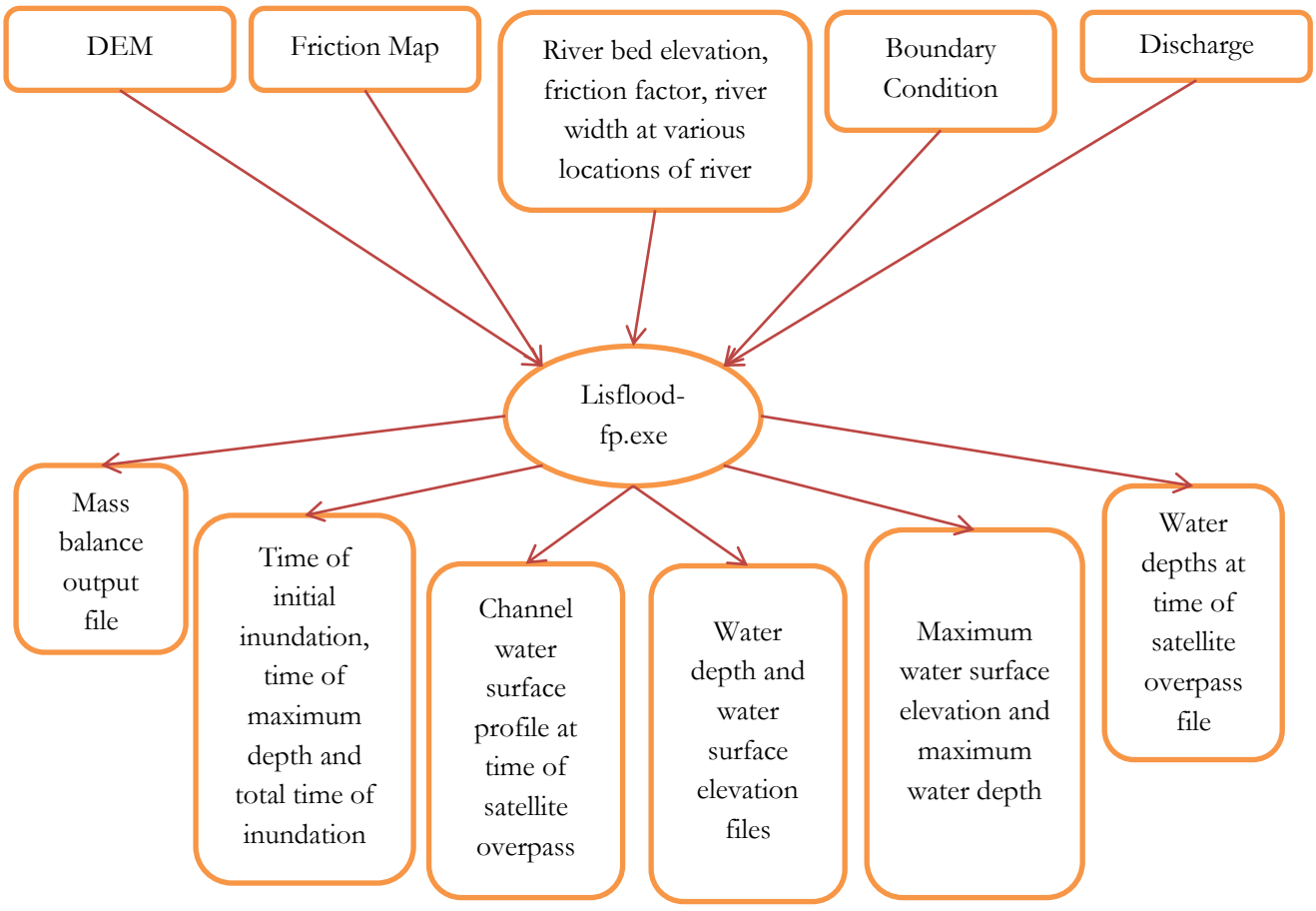

Figure 17: Various Inputs and output of Lisflood-fp as described in manual.

5.1. Preparing Observed Flood Map

The Water Cover Area (WCA) map prepared by slicing operation on SAR image dose not truly represents the flooded area. It also includes the permanent water bodies. These permanent water bodies have to be extracted from LULC map. Permanent Water Body (PWB) map will be resampled to resolution of Radarsat-1 image.

In Erdas Imagine model maker the conditional statement will be ran that if any pixel in PWB map is water then change the same pixel in WCA to non-flooded (i.e. dry) otherwise keep the WCA image as it is. So, the flood map will be ready. The method is explained graphically in **Error! Reference source not found.**.

5.2. 'Fit Value' Measure of performance of results

The performance of simulation results was measured by term 'Fit' and 'Overall Accuracy'. For this, following contingency table is populated.

Table 6: Contingency table for Fit value Calculation

	Observed- Flooded	Observed- Non flooded
Model- Flooded	A= Both flooded	B=Predicted Flooded but Observed Non flooded
Model- Non Flooded	C= Predicted Non flooded but Observed Flooded	D=Both Non flooded

Area (m^2) in each category i.e. A, B, C and D can be obtained by overlapping observed flood map and predicted flood map on one another. For 'Fit' is calculated as:

$$F = D/(B + C + D)$$

It divides the correctly predicted floodplain pixels to total no. of flood plain pixels. Its calculation does not include correctly predicted non flooded pixels which can bias the calculations. Fit value varies from zero to one. Fit value near to zero indicates bad overlap and vice versa.
The overlap was also measured by Overall Accuracy. It is ratio of correctly predicted area to total area.

$$(Accuracy)_{overall} = (A + D)/(C + D)$$

6. RESULTS AND DISCUSSION

6.1. Discharge in Dhanua river by HEC-RAS

Hydrograph of discharge at Balianta Gauging Station is shown in Figure 11. This was given as input to HEC-RAS. By using various cross sections along the river the water surface elevation was calculated. The elevation of escape was measured on field as 19.51. The difference between elevation of escape and water surface provided us the water depth flowing over the escape. These water surface elevation and escape elevation are shown in Figure 18.

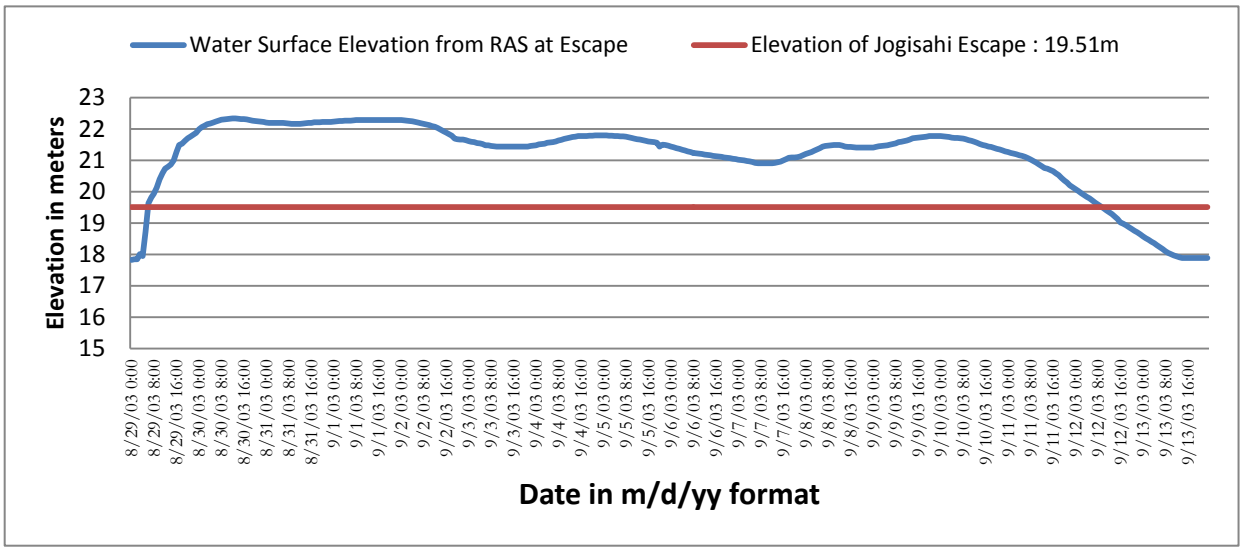

Figure 18: Water surface elevation calculated by HEC-RAS model at cross-section near Jogisahi Escape

The water depth flowing over escape is the difference between water surface elevation at Jogisahi escape and its elevation. The method to get discharge from water depth is described in section 5.2. The resulted discharge hydrograph is shown in Figure 11.

6.2. Flood Plain Inundation Modeling using "Lisflood-fp"

The 'Lisflood-fp' hydrodynamic inundation model was simulated using various resolutions DEM and other freely available topographic model. Water depth map produced in result was used to measure the accuracy of model. In this water depth map, area having water depth less than 0.2m was considered as non-flooded and above it as flooded.

6.2.1. Various Resolution DEM

The Figure 19 shows overlay of predicted flood map produced by using 6m resolution DEM over observed flood extent. It is showing the inundation is seen evenly along the both side of river. This overlap image was used to populate contingency table shown in Table 7. This shows overall accuracy was measured to be 0.63 and fit value as 0.17.

The Figure 20 shows overlay of predicted flood map produced by using 10m resolution DEM over observed flood extent. It is seen that similar to previous overlay, inundation is evenly along the both side of river with greater distance. This overlap image was used to populate contingency table shown in

Table 8. This shows overall accuracy was measured to be 0.64 and fit value as 0.25.

The Figure 20Figure 21 shows overlay of predicted flood map produced by using 20m resolution DEM over observed flood extent. It is seen that similar to previous overlay, inundation is evenly along the both side of river with greater distance and it is increasing as the resolution becoming courser. This overlap image was used to populate contingency table shown in Table 9. This shows overall accuracy was measured to be 0.68 and fit value as 0.39.

The effect was similar using 30m resolution and 60 m resolution DEM shown in Figure 22 and Figure 23.

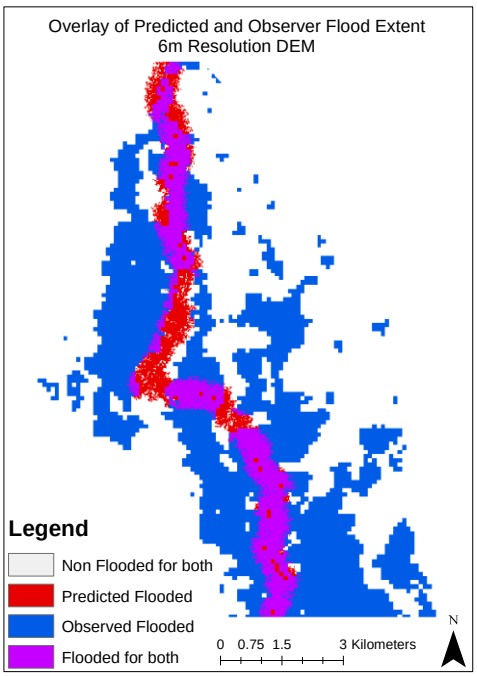

Figure 19: Overlay of predicted flood map produced by using 6m resolution DEM over Observed Flood Extent 4th Sep 2003 12:20:05 Hrs.

Table 7: Contingency table populated with area in m^2 using overlay of predicted and observed flood map for 4th Sep 2003 12:20:05 Hr. using 6m resolution DEM (all values)

6m resolution DEM			
	Observed Non-Flooded	Observed flooded	Row Total
Predicted Non-Flooded	4470264	2709396	7179660
Predicted Flooded	306684	620316	927000
Column Total	4776948	3329712	8106660
	Overall Accuracy	0.63	
	Fit (F)	0.17	

For overlay analysis using 30m and 60m resolution, overall accuracy was measured to be 0.69 and 0.60 respectively. Fit values for both were same as 0.47. Their contingency tables are shown in Table 10 and Table 11.

The Figure 20Figure 24 shows overlay of predicted flood map produced by using 90m resolution DEM over observed flood extent. It is seen that all the discharge is consumed for inundating the upper catchment area and

no water is able to reach the downstream end. Hence accuracy of prediction was severely affected. In Table 12, its overall accuracy was measured to be 0.48 and fit value as 0.26.

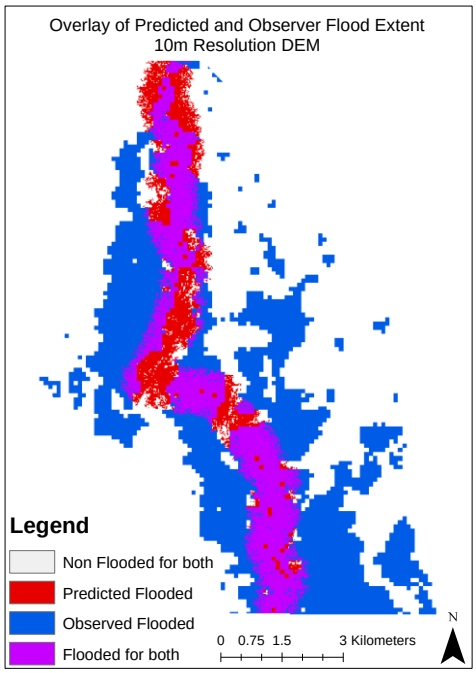

Figure 20: Overlay of predicted flood map produced by using 10m resolution DEM over Observed Flood Extent 4th Sep 2003 12:20:05 Hrs.

Table 8: Contingency table populated with area in m^2 by using overlay of predicted and observed flood map for 4th Sep 2003 12:20:05 Hr. using 10m resolution DEM

10m resolution DEM			
	Observed Non-Flooded	Observed flooded	Row Total
Predicted Non-Flooded	11915300	6658900	18574200
Predicted Flooded	1333800	2604200	3938000
Column Total	13249100	9263100	22512200
	Overall Accuracy	0.64	
	Fit (F)	0.25	

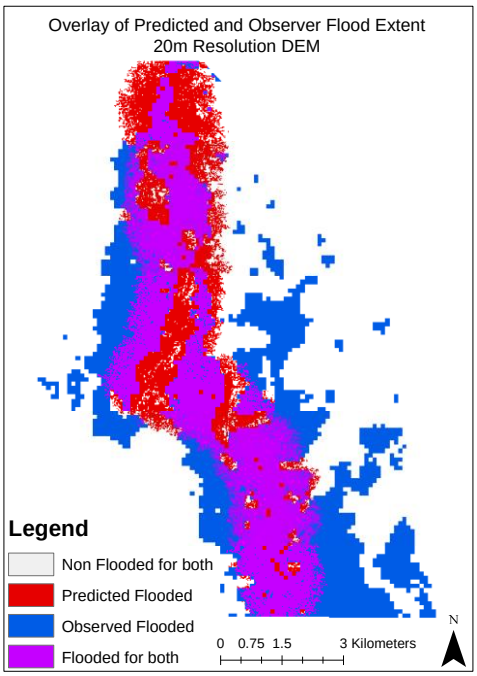

Figure 21: Overlay of predicted flood map produced by using 20m resolution DEM over Observed Flood Extent 4th Sep 2003 12:20:05 Hrs.

Table 9: Contingency table populated with area in m² by using overlay of predicted and observed flood map for 4th Sep 2003 12:20:05 Hr. using 20m resolution DEM

20m resolution DEM			
	Observed Non-Flooded	Observed flooded	Row Total
Predicted Non-Flooded	42954800	18858000	61812800
Predicted Flooded	10032000	18249600	28281600
Column Total	52986800	37107600	90094400
	Overall Accuracy	0.68	
	Fit (F)	0.39	

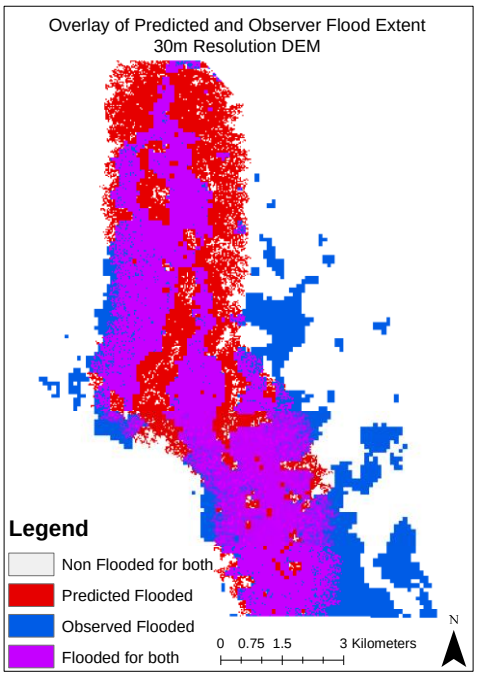

Figure 22: Overlay of predicted flood map produced by using 30m resolution DEM over Observed Flood Extent 4th Sep 2003 12:20:05 Hrs.

Table 10: Contingency table populated with area in m^2 by using overlay of predicted and observed flood map for 4th Sep 2003 12:20:05 Hr. using 30m resolution DEM

30m resolution DEM			
	Observed Non-Flooded	Observed flooded	Row Total
Predicted Non-Flooded	37961100	12842100	50803200
Predicted Flooded	15000300	24239700	39240000
Column Total	52961400	37081800	90043200
	Overall Accuracy	0.69	
	Fit (F)	0.47	

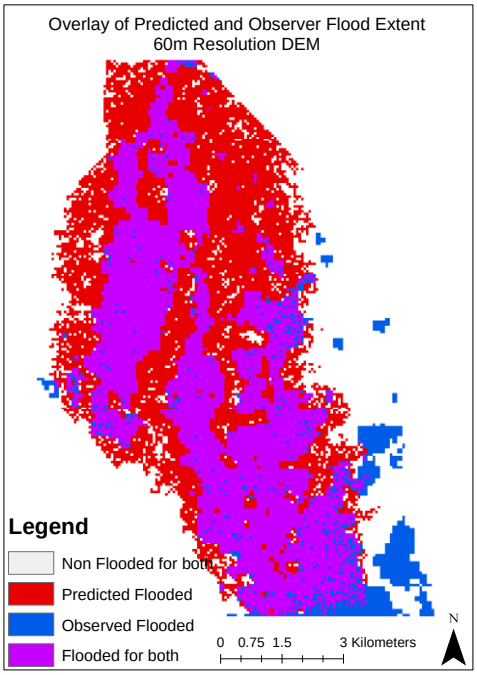

Figure 23: Overlay of predicted flood map produced by using 60m resolution DEM over Observed Flood Extent 4th Sep 2003 12:20:05 Hrs.

Table 11: Contingency table populated with area in m^2 by using overlay of predicted and observed flood map for 4th Sep 2003 12:20:05 Hr. using 60m resolution DEM

60m resolution DEM			
	Observed Non-Flooded	Observed flooded	Row Total
Predicted Non-Flooded	22874400	5799600	28674000
Predicted Flooded	29833200	31219200	61052400
Column Total	52707600	37018800	89726400
	Overall Accuracy	0.60	
	Fit (F)	0.47	

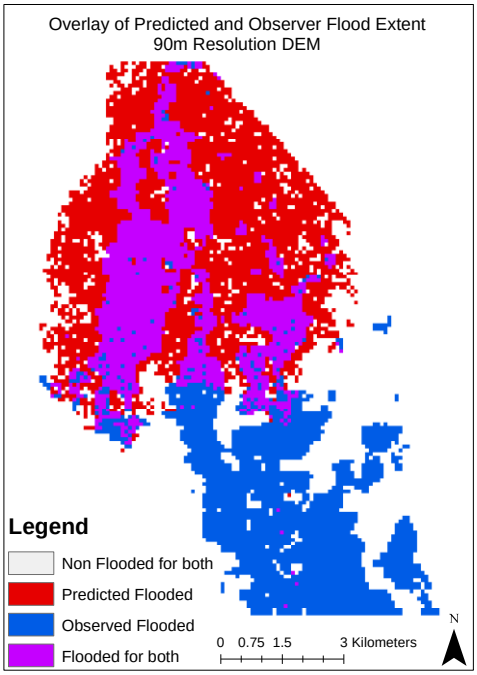

Figure 24: Overlay of predicted flood map produced by using 90m resolution DEM over Observed Flood Extent 4th Sep 2003 12:20:05 Hrs.

Table 12: Contingency table populated with area in m^2 by using overlay of predicted and observed flood map for 4th Sep 2003 12:20:05 Hrs. using 90 m resolution DEM

90m resolution DEM			
	Observed Non-Flooded	Observed flooded	Row Total
Predicted Non-Flooded	27175500	20541600	47717100
Predicted Flooded	25660800	16135200	41796000
Column Total	52836300	36676800	89513100
	Overall Accuracy	0.48	
	Fit (F)	0.26	

6.2.2. Freely available DEM

The Figure 25 shows overlay of predicted flood map produced by using ASTER DEM over observed flood extent for 4th Sep. 2003 12:20:05 Hrs. It is showing some extra inundation at opening of stream else much of the inundation is in the observed limits. It can be seen that much of the water is getting drained out of DEM extent. It is not following the pattern of inundation which was seen in case of stereo pair generated DEM. Water is not showing the tendency to exclusively inundate the adjacent the area adjoining the stream line. This overlap image was used to populate contingency table shown in Table 13. This shows overall accuracy was measured to be 0.62 and fit value as 0.19.

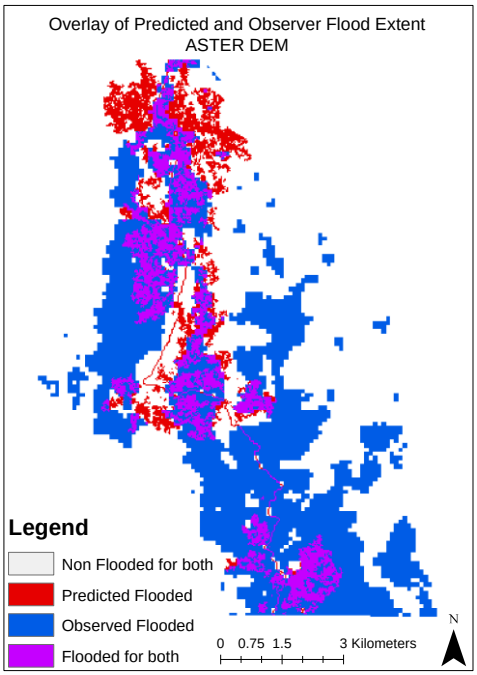

Figure 25: Overlay of predicted flood map produced by using ASTER 30m resolution DEM over Observed Flood Extent 4th Sep 2003 12:20:05 Hrs.

Table 13: Contingency table populated with area in m^2 by using overlay of predicted and observed flood map for 4th Sep 2003 12:20:05 Hr. using ASTER DEM 30m resolution DEM

ASTER DEM			
	Observed Non-Flooded	Observed flooded	Row Total
Predicted Non-Flooded	47646000	28845900	76491900
Predicted Flooded	5315400	8235900	13551300
Column Total	52961400	37081800	90043200
	Overall Accuracy	0.62	
	Fit (F)	0.19	

The Figure 26 shows overlay of predicted flood map produced by using CARTOSAT DEM over observed flood extent for 4th Sep. 2003 12:20:05 Hrs. There was an issue with this DEM that elevation values were negative. Hence, an offset was given to whole DEM of 65.5 m. So that mean of range of SRTM DEM and CARTOSAT DEM is same. In this case much of discharge is drained out of the study area. The inundation predicted is within the observed flood extent but too less. Its effect can be seen on accuracy measurements. This overlap image was used to populate contingency table shown in Table 14. This shows overall accuracy was measured to be 0.62 and fit value as 0.09.

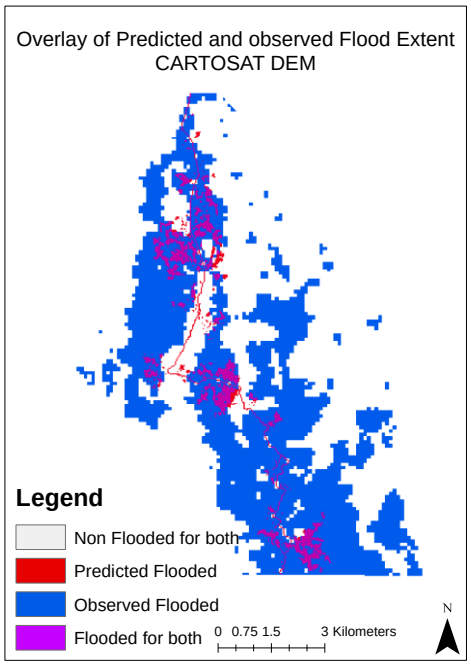

Figure 26: Overlay of predicted flood map produced by using CARTOSAT DEM 30m resolution DEM over Observed Flood Extent 4th Sep 2003 12:20:05 Hrs.

Table 14: Contingency table populated with area in m² by using overlay of predicted and observed flood map for 4th Sep 2003 12:20:05 Hr. using CARTOSAT DEM 30m resolution DEM

CARTOSAT DEM			
	Observed Non-Flooded	Observed flooded	Row Total
Predicted Non-Flooded	52492500	33658200	86150700
Predicted Flooded	615600	3429900	4045500
Column Total	53108100	37088100	90196200
	Overall Accuracy	0.62	
	Fit (F)	0.09	

The Figure 27 shows overlay of predicted flood map produced by using SRTM DEM over observed flood extent for 4th Sep. 2003 12:20:05 Hrs. Here inundation predicted is seen in good agreement with observed one. Some extra inundation is predicted in upstream region as compared to downstream. This overlap image was used to populate contingency table shown in Table 15. This shows overall accuracy was measured to be 0.65 and fit value as 0.37.

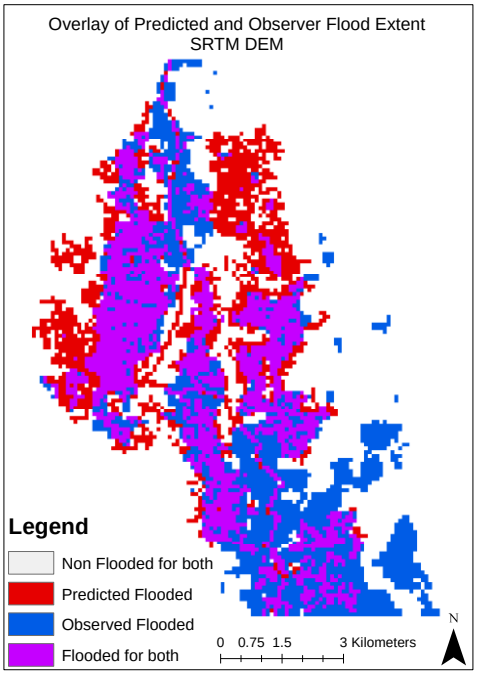

Figure 27: Overlay of predicted flood map produced by using SRTM DEN 90m resolution DEM over Observed Flood Extent 4th Sep 2003 12:20:05 Hrs.

Table 15: Contingency table populated with area in m² by using overlay of predicted and observed flood map for 4th Sep 2003 12:20:05 Hr. using SRTM DEM 90m resolution DEM

SRTM DEM			
	Observed Non-Flooded	Observed flooded	Row Total
Predicted Non-Flooded	38645100	17739000	56384100
Predicted Flooded	12360600	17787600	30148200
Column Total	51005700	35526600	86532300
	Overall Accuracy	0.65	
	Fit (F)	0.37	

6.3. Discussion

The overlap measurements for predictions using various resolutions DEM are shown graphically in Figure 28. It shows that accuracy of predictions went on decreasing as resolution became coarser. As it was seen in overlay maps, predictions were following a pattern of getting flooded over flood plain more easily than flowing through stream. Hence, at coarser resolution water was getting accumulated inside the study area. It must be noted that only three GCP were used for generating DEM hence its accuracy is less. If in future more accurate DEM is generated than the results will improve.

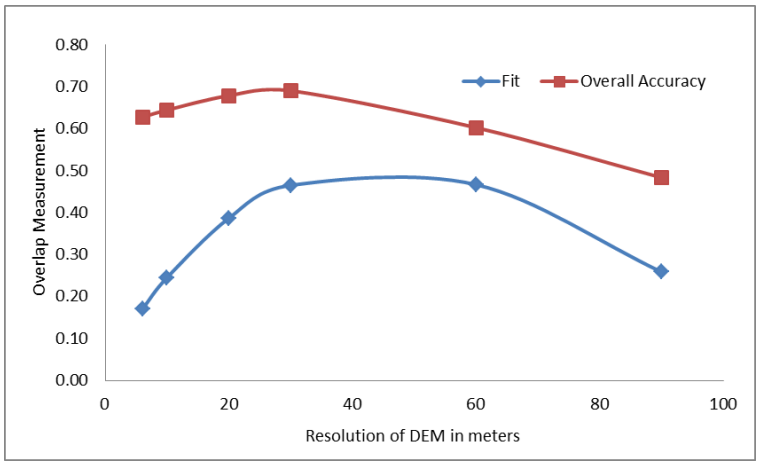

Figure 28: Variation in Overall Accuracy and Fit value w.r.t. change of resolution of DEM

Fit values for predicted inundation extent by various freely available DEM are arranged in a Table 16 below. In overlaid flood maps of ASTER and CARTOSAT inundation was very less and discharge was flowing out of study area. Hence, their accuracy was measured poor.

The overlay flood map of SRTM DEM was having higher overall accuracy and fit values. The predicted flood map was in good agreement with the observed one. The additional floods were predicted in upper region of study area. Fewer floods were predicted in downward region. This is because higher friction factors given to flood plain. For improving the accuracy of predictions fine calibration of this flood plain friction is needed.

The SRTM DEM is been corrected with various techniques to obtain hydrological correct DEM. The SRTM DEM was converted to contours and points. Area around missing values was interpolated using TOPOGRID algorithm. It is based upon algorithms of Hutchinson (1988: 1989) to use contour data to produce hydrological sound DEM.

Table 16: Overlap measurement using Overlap Accuracy and Fit value for various freely available DEM.

Freely Available DEM	Overall Accuracy	Fit
ASTER DEM	0.62	0.19
CARTOSAT DE	0.62	0.09
SRTM DEM	0.65	0.37

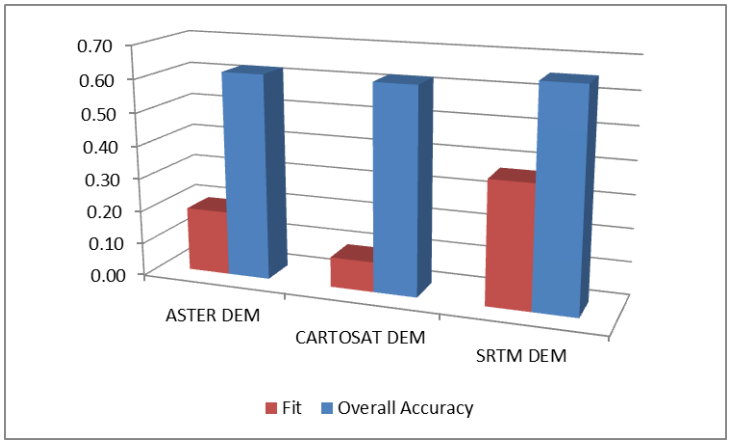

Figure 29: Bar diagram of Overlap measurements (i.e. Overlap Accuracy and Fit value) for ASTER, CARTOSAT and SRTM DEM.

7. CONCLUSION, LIMITATIONS AND RECOMMENDATIONS

7.1. Conclusion

7.1.1. What is the accuracy of model simulations with SAR data?

Vertical accuracy of SRTM was highest of all DEM used. The DEM used was of version 4. It was corrected for most of the corrections which are desired for hydrological processing. These corrections were like removing voids, removing cliffs at the joint of tile, removal of costal lines and using different interpolation techniques and algorithms to fill void. The inundation produced by model was having overall accuracy of 65% and fit value of 37%.

7.1.2. What are the changes in simulated inundation area due to change in DEM of different resolution?

Area of inundation shown by Lisflood-fp was increasing as the resolution of input DEM was decreasing. This observation is similar to the conclusion of (Aaron Cook 2009) while working on FESWMS 2DH model. But the inundation maps generated are not in according to flood map. Hence, resolution of DEM is not making any difference to get good inundation maps.

Quality of the DEM has to be good to get better inundation. As it was seen no proper inundation was generated with the help of Cartosat-1 and ASTER. Since, they were not corrected for voids and missing values, whereas for SRTM DEM various interpolation techniques were applied for removing voids and missing values. Its vertical accuracy is less than 16m with 90% confidence, less than all other elevation data. Hence, resolution dose not play major role but vertical accuracy is more important for better flood inundation maps.

7.2. Limitations

- Bed elevation data used is not of adequate accuracy.
- Resolution of SAR image for validation is too large as compared to fine resolution of DEM.

7.3. Recomendations

- With temporal multispectral images urban area and rice fields can be mapped. This will help damage assessment of urban area and rice fields.
- Resolution of SAR image used will affect the validation of model. Hence, microwave image of finer resolution must be used for validation.
- More realistic bed elevation values can be used.
- Correction for tree height can be given to DEM. It will give bare earth DEM.
- Tree height and surface roughness can be extracted from remote sensing techniques like microwave. This will reduce dependence on field data.
- Methodology has to be developed to make Cartosat-1 data more usable for hydrological processing.

8. REFFERENCES

Aaron Cook, V. M. (2009). "Effect of topographic data, geometric configuration and modeling approach on flood inundation mapping." Journal of Hydrology **377**(131–142).

Arcement, G. J. and V. R. Schneider (1989). Guide for selecting Manning's roughness coefficients for natural channels and flood plains, US Government Printing Office.

Bates, P. D. and A. P. J. De Roo (2000). "A simple raster-based model for flood inundation simulation." Journal of Hydrology **236**(1): 54-77.

Bates PD, L. S. a. F. R. (2005). Front Matter. Computational Fluid Dynamics, John Wiley & Sons, Ltd**:** i-viii.

The prelims comprise: * Half-Title Page * Title Page * Copyright Page * Table of Contents * List of Contributors

Bates, P. D., et al. (2006). "Reach scale floodplain inundation dynamics observed using airborne synthetic aperture radar imagery: Data analysis and modelling." Journal of Hydrology **328**(1–2): 306-318.

Guha-Sapir, D., et al. (2011). "Annual disaster statistical review 2010." Centre for Research on the Epidemiology of Disasters.

Horritt, M. S. and P. D. Bates (2001). "Effects of spatial resolution on a raster based model of flood flow." Journal of Hydrology **253**(1–4): 239-249.

Horritt, M. S. and P. D. Bates (2001a). "Predicting floodplain inundation: raster-based modelling versus the finite-element approach." Hydrological Processes **15**(5): 825-842.

Hunter, N. M., et al. (2008). "Benchmarking 2D hydraulic models for urban flooding." Proceedings of the ICE-Water Management **161**(1): 13-30.

Hunter, N. M., et al. (2005). "An adaptive time step solution for raster-based storage cell modelling of floodplain inundation." Advances in Water Resources **28**(9): 975-991.

Merwade, V., et al. (2008). "GIS techniques for creating river terrain models for hydrodynamic modeling and flood inundation mapping." Environmental Modelling & Software **23**(10â€“11): 1300-1311.

Mukherjee, S., et al. (2013). "Evaluation of vertical accuracy of open source Digital Elevation Model (DEM)." International Journal of Applied Earth Observation and Geoinformation **21**(0): 205-217.

Muralikrishnan, S., et al. (2013). "Validation of indian national DEM from Cartosat-1 data." Journal of the Indian Society of Remote Sensing **41**(1): 1-13.

Neal, J., et al. (2012). "A subgrid channel model for simulating river hydraulics and floodplain inundation over large and data sparse areas." WATER RESOURCES RESEARCH **48**(11).

Rexer, M. and C. Hirt (2014). "Comparison of free high resolution digital elevation data sets (ASTER GDEM2, SRTM v2.1/v4.1) and validation against accurate heights from the Australian National Gravity Database." Australian Journal of Earth Sciences **61**(2): 213-226.

Sanders, B. F., et al. (2010). "ParBreZo: A parallel, unstructured grid, Godunov-type, shallow-water code for high-resolution flood inundation modeling at the regional scale." Advances in Water Resources **33**(12): 1456-1467.

Schumann, G. P., et al. (2013). "A first largeâ€ • scale flood inundation forecasting model." WATER RESOURCES RESEARCH **49**(10): 6248-6257.

Sciusco, L. R. F. (2012). Italy-From Business Continuity to Service Continuity-The Case of the Italian Financial System. Improving the Assessment of Disaster Risks to Strengthen Financial Resilience. G2012 MEXICO, Government of Mexico and the World Bank Group**:** 177-190.

Stoesser, T., et al. (2003). "Application of a 3D numerical model to a river with vegetated floodplains." Journal of Hydroinformatics **5**: 99-112.

Subramanya, K. (2007). Flow in Open Channels, Tata McGraw-Hill Education.

Sushanta Kumar Jata, M. N., Nibedita Jata (2011). Flood and Risk Management Strategy in Orissa. Orissa Review. Bhuvaneshwar, Dept. of Information and Public Relation, Govt. of Orissa**:** 62-67.

Tachikawa, T., et al. (2011). "ASTER Global Digital Elevation Model Version 2–Summary of Validation Results August 31, 2011."

Trigg, M. A., et al. (2009). "Amazon flood wave hydraulics." Journal of Hydrology **374**(1): 92-105.

Werner, M. G. F. (2004). Spatial flood extent modelling. A performance based comparison, Delft University Press.

Wilson, M., et al. (2007). "Modeling large-scale inundation of Amazonian seasonally flooded wetlands." Geophysical Research Letters **34**(15): L15404.

WRIS, I. (2012). River Basin Atlas of India, RRSC-West, NRSC, ISRO, Jodhpur, India.

Yamazaki, D., et al. (2012). "Adjustment of a spaceborne DEM for use in floodplain hydrodynamic modeling." Journal of Hydrology **436–437**(0): 81-91.

APPENDIX A

Accuracy report of supervised classification:

CLASSIFICATION ACCURACY ASSESSMENT REPORT

Image File : d:/classify/3class.img
User Name: Piyush
Date : Tue Mar 11 18:36:13 2014

ERROR MATRIX

	Reference Data			
Classified Data	Unclassifi			
Unclassified	0	0	0	0
	0	0	0	0
	0	0	0	0
	0	0	0	0
	0	0	0	0
felloland	0	0	0	0
	0	0	0	0
treecoverrural_	0	0	0	0
	0	0	0	0
	0	0	0	0
	0	0	0	0
	0	0	0	0
	0	0	0	0
	0	0	0	0
	0	0	0	0
WaterBody	0	0	0	0
Column Total	0	0	0	0

	Reference Data			
Classified Data	felloland			treecoverr
Unclassified	0	0	0	0
	0	0	0	0
	0	0	0	0
	0	0	0	0
	0	0	0	0

felloland	0	16	0	2
	0	0	0	0
treecoverrural_	0	1	0	1
	0	0	0	0
	0	0	0	0
	0	0	0	0
	0	0	0	0
	0	0	0	0
	0	0	0	0
	0	0	0	0
WaterBody	0	0	0	0
Column Total	0	17	0	3

	Reference Data			
Classified Data				
Unclassified	0	0	0	0
	0	0	0	0
	0	0	0	0
	0	0	0	0
	0	0	0	0
felloland	0	0	0	0
	0	0	0	0
treecoverrural_	0	0	0	0
	0	0	0	0
	0	0	0	0
	0	0	0	0
	0	0	0	0
	0	0	0	0
	0	0	0	0
	0	0	0	0
WaterBody	0	0	0	0
Column Total	0	0	0	0

	Reference Data			
Classified Data				WaterBody
Unclassified	0	0	0	0
	0	0	0	0
	0	0	0	0
	0	0	0	0
	0	0	0	0
felloland	0	0	0	0
	0	0	0	0

treecoverrural_	0	0	0	0
	0	0	0	0
	0	0	0	0
	0	0	0	0
	0	0	0	0
	0	0	0	0
	0	0	0	0
	0	0	0	0
WaterBody	0	0	0	0
Column Total	0	0	0	0

----- End of Error Matrix -----

ACCURACY TOTALS

Class Name	Reference Totals		Classified Totals	Number Correct	Producers Accuracy	Users Accuracy
Unclassified	0	0	0	---	---	
	0	0	0	---	---	
	0	0	0	---	---	
	0	0	0	---	---	
	0	0	0	---	---	
fell land	17	18	16	94.12%		88.89%
	0	0	0	---	---	
treecoverrural_	3	2	1	33.33%		50.00%
	0	0	0	---	---	
	0	0	0	---	---	
	0	0	0	---	---	
	0	0	0	---	---	
	0	0	0	---	---	
	0	0	0	---	---	
	0	0	0	---	---	
WaterBody	0	0	0	---	---	
Totals	20	20	17			

Overall Classification Accuracy = 85.00%

----- End of Accuracy Totals -----

KAPPA (K^) STATISTICS

Overall Kappa Statistics = 0.3182

Conditional Kappa for each Category.

Class Name	Kappa
Unclassified	0.0000
	0.0000
	0.0000
	0.0000
	0.0000
felloland	0.2593
	0.0000
treecoverrural_settlement	0.4118
	0.0000
	0.0000
	0.0000
	0.0000
	0.0000
	0.0000
	0.0000
WaterBody	0.0000

----- End of Kappa Statistics -----